Arch. Metall. Mater. **71** (2026), 3, 923-932

DOI: https://doi.org/10.24425/amm.2026.1984

MARCIN KASZUBA[1], MARZENA LACHOWICZ[1], PAWEŁ WIDOMSKI[1], PAWEŁ KUSTROŃ[1], TOMASZ RZADKOSZ[1], PAWEŁ SOKOŁOWSKI[1], ZBIGNIEW GRONOSTAJSKI[1*]

APPLICATION OF NUMERICAL MODELING TO DETERMINE THE PARAMETERS OF THE HARDFACING PROCESS AND TO DETERMINE THE PROPERTIES OF THE OBTAINED HARDFACING LAYERS OF FORGING DIES

A numerical analysis of the hardfacing process was conducted to precisely define its technological parameters, which were then experimentally verified. The developed numerical models demonstrated high consistency with the experimental results, confirming their suitability for analyzing and selecting key parameters of the hardfacing process. The use of a simulation approach significantly reduced the number of time-consuming and costly experimental tests and allowed for a better understanding of the phenomena occurring during regenerative hardfacing. The research was supplemented with a description of the microstructural phenomena occurring in the weld.

Keywords: Hardfacing; forging; tools

1. Introduction

The forging industry currently plays a crucial role worldwide, as it is closely linked to numerous industrial sectors, particularly the automotive, mechanical engineering and railway industries. Current market trends are not only focused on price reductions but also on improving quality and increasing product diversity in ever-smaller production runs. It demands improved forging tool quality and the development of remanufacturing methods [1].

The aim of this research was to develop regenerative hardfacing technology for forging tools used in die forging processes. This technology will contribute to increased tool durability, efficiency, and accuracy in forging production. Die inserts made of expensive tool steels, previously destined for scrap after use, can now be regenerated and reused [2].

One of the most important measures of a production tool's quality is its reliability. This indicates its ability to operate for long periods without failure, and is therefore closely linked to its durability. It is often assumed that tool durability is measured by the number of operations that can be performed with the tool to produce products of the required quality [3]. The durability of tools used in industrial manufacturing processes is a key factor determining the efficiency of a given production process [4].

Metal forming processes are one of the most sophisticated groups of manufacturing processes, characterized by low tool durability. This is particularly evident in hot die forging, where tools are simultaneously subjected to three main factors causing their deterioration: intense thermal shocks, cyclically varying mechanical loads and intense friction. These factors cause a variety of destructive phenomena on the tool surface during use. Research indicates the presence of wear mechanisms such as abrasive wear, thermomechanical fatigue, plastic deformation, fatigue cracking, adhesive wear and oxidation [5].

Research focuses primarily on the wear mechanisms occurring in the surface layer of tools and on methods for increasing their resistance to these mechanisms. The available literature provides information on destructive phenomena, with varying classifications of these mechanisms. It is most commonly assumed that, statistically, 70% of forging dies are withdrawn from production due to dimensional loss – due to abrasive wear and plastic deformation – and 25% due to fatigue cracks, and only 5% for other reasons (non-compliance with technology, design or material defects, or defects in heat and thermochemical treatment, etc.) [6]. In reality, many of these phenomena often occur simultaneously, and the relationships between them depend primarily on the conditions of the forging process, proper tool design and manufacture, appropriate heat treatment for the selected tool material, the shape of the blank and/or forging, etc. [3].

Hot forging steel products requires heating the material to temperatures of 1000-1200°C, with the tool surface temperature

[1] WROCŁAW UNIVERSITY OF SCIENCE AND TECHNOLOGY, CENTER FOR MATERIALS ENGINEERING AND METAL FORMING, METAL FORMING, WELDING AND METROLOGY DEPARTMENT, WYBRZEŻE STANISŁAWA WYSPIAŃSKIEGO 27, 50-370 WROCŁAW, POLAND

[*] Corresponding author: zbigniew.gronostajski@pwr.edu.pl

reaching up to 800°C, followed by rapid cooling. The dominant tool wear mechanism under these conditions is thermomechanical fatigue [7], with other wear mechanisms intensified by the tool operating temperature [8,9].

One of the most commonly used methods for creating layers with increased wear resistance is hardfacing. Regenerative hardfacing is most often used to regenerate worn forging dies. This involves removing a layer of material from the surface and covering it with a new layer composed of melted substrate material and weld metal. The purpose of the hardfacing layer is to ensure the best possible operational properties of the surface layer. This can be a preventative or, in the case of regenerative hardfacing, to restore these properties by rebuilding the surface. Hardfacing of forging tools can be performed using various welding methods: coated electrodes, self-shielded flux-cored wire, submerged arc, MIG (solid wire or flux-cored wire), TIG and laser [10]. All of these methods can be considered effective, but they differ in terms of efficiency, precision of weld bead placement, process control and robotic capabilities, and the ability to use a variety of additional materials (weld metals) [11]. Hardfacing offers almost unlimited possibilities for adding a wide range of alloying additives to the surface layer and enables the application of layers with a complex structure or the creation of zones with local properties and special resistance [12].

In practice, MAG/MIG hardfacing with solid or flux-cored wire is the most commonly used method. This is a highly efficient method, and there are numerous examples confirming its effectiveness in increasing the durability of forging tools [13]. This hardfacing can be performed in two stages: initial filling with filler metal (rebuilding), depositing an intermediate layer, and then surface hardening with a layer with enhanced mechanical properties (hardfacing) [14]. Numerous examples of tool durability improvements through hardfacing are known [15], and it is considered one of the most popular and effective methods available [16].

A well-established method is hardfacing with a coated electrode. This method allows for manual or semi-automatic hardfacing using simple manipulators. Since the mid-20th century, hardfacing by "flooding" the die cavity has been widely used, using electrodes developed and marketed by the firm Weld Mold [17]. This is a highly efficient method, as the deposited weld metal can reach up to 45 kg/h. This method is also successfully used for local regenerative repairs [18]. Its main drawback is the difficulty in robotizing it, which is why it is increasingly being replaced by MIG, MAG, and laser cladding.

Among welding techniques, the TIG method is noteworthy, providing a stable arc, a small weld pool, and no spatter. The resulting deposit is pore-free and has a more uniform structure and properties. TIG surfacing is characterized by lower productivity but improved functional properties of the deposited welds. The TIG method is used to increase the durability of forging tools by hardfacing with Stellites (cobalt-or nickel-based superalloys) [19].

There are many other applications where hardfacing has improved the durability of forging tools. Selective hardfacing, which involves the localized introduction of a material with different properties to counteract wear in a specific area [20]. Hardfacing can be performed in zones [21] or layers by building a gradient and bimetallic layers [22,23].

Among the new trends in regeneration, a valuable method is plasma hardfacing (PTA), which is extremely precise, allows for modification of the chemical composition of the weld by changing the powder composition, allows for precise control of the process energy and leads to obtaining a low degree of mixing, which gives the expected composition of the weld even in the first layer [24].

The latest solutions using additive techniques enable a semi-automated process in which regenerative welding is performed using systems such as MaxQ Repair provided by RAMLAB [25]. These methods utilize a welding arc, laser energy, or plasma as a power source. Their advantage is reduced material consumption and repair time by limiting machining allowances [26,27].

In recent years, numerical modeling has played an increasingly important role in improving regenerative hardfacing processes [28]. It enables the analysis of thermal, mechanical, and metallurgical phenomena occurring during layer deposition [29]. The use of finite element methods enables the prediction of temperature distribution, residual stresses, deformation, and heat-affected zones, thereby reducing the need for costly experimental tests and shortening technology development time [30]. In the case of forging tool repair, the ability to simulate the impact of process parameters on joint quality, material mixing, and the risk of weld imperfections is particularly important, which facilitates the selection of more stable and repeatable technological variants [31]. Numerical modeling can also be useful in designing multi-layer hardfacing welds with diverse properties, predicting the durability of regenerated components, and supporting robotization and automation of the regenerative process [32]. Consequently, it is an important tool supporting the development of modern hardfacing technologies, especially in applications requiring high reliability and precision.

As part of this research, a numerical analysis of the hardfacing process was conducted to precisely define its technological parameters, which were then experimentally verified. The developed numerical models demonstrated high consistency with the experimental results, confirming their suitability for analyzing and selecting key parameters of the hardfacing process. The use of a simulation approach significantly reduced the number of time-consuming and costly experimental tests and allowed for a better understanding of the phenomena occurring during regenerative hardfacing.

2. Methodology

2.1. Subject of research

The study focused on axisymmetric forging tools. These included various types of forging dies, each with varying geometric complexity. One of the largest groups of tools comprises hammer forging dies, typically made of 55NiCrMoV6 steel. These are typically large tools, which, due to their significant production costs, require repeated regeneration by either lowering the impression or hardfacing. The forging process requires regeneration across the entire surface in contact with the hot metal by weld overlays.

Axially symmetric samples, similar to die inserts, made of 55NiCrMoV6 steel, with a diameter of 300 mm and a height of 100 mm, were selected as the subject of the study. From the perspective of the phenomena occurring during regenerative hardfacing, such samples can be considered representative as long as the interpass temperature of hardfacing is maintained at a level similar to that occurring during the hardfacing process of larger dies. The chemical composition of the steel is presented in TABLE 1

TABLE 1

Chemical composition of the tested steel

Element	C	Ni	Cr	Mo	V	Fe
Content [%]	0,56	1,75	1	0,5	0,1	balance

The selection of the filler metal, a flux-cored wire, as the weld metal was based on commonly accepted criteria to ensure that its properties did not differ significantly from those of the material itself. The proposed material was EnDOtec DO*04, a flux-cored wire with a metal core that produces a weld deposit with a martensitic structure typical of stainless steels. It is characterized by high resistance to pressure and impact, corrosion, and oxidation up to 550-650°C. The hardness of the weld deposit increases during operation through a precipitation hardening mechanism. The chemical composition of the filler material used is presented in TABLE 2.

TABLE 2

Chemical composition of substrate materials used for hardfacing

Element	C	Mn	Si	S	P	Cr	Mo	Ni	V	Fe
Content [%]	0.6	0.72	0.23	0.005	0.009	0.97	0.43	1.71	0.08	balance

2.2. Numerical modeling

2.2.1. Simplified model

To select the appropriate parameters for a given process, a simplified model of the process was created in the Simufact program. Numerical studies of the regenerative hardfacing process were conducted using the finite element method. Work began with developing models for simple geometric samples measuring 100×100×50 mm and two welded layers. The primary analysis focused on the temperature field distribution and penetration depth for a selected group of process parameters. This enabled the definition of a narrow range of parameters, which were experimentally used to model complex geometry to verify the bead geometry and quality.

Numerical studies were conducted for various hardfacing parameters (welding current Is ranging from 180 to 280 A and welding torch travel speed Vs ranging from 20 to 40 cm/min) to initially narrow the range of parameters used during the experiments. At this stage, the focus was on analyzing the temperature field distribution in the hardfacing area and assessing the area of weld penetration into the base material. Failure to reach the melting point in any of the welded areas could potentially indicate a lack of fusion, while reaching the melting point of the substrate material across the entire width of the weld indicates the formation of a homogeneous joint and confirms the correct selection of hardfacing parameters. Fig. 1 presents selected results of numerical calculations with the fusion geometry.

The analysis revealed that for a welding current of $Is = 180$ A, full penetration was not achieved, both between the layers and with the substrate (Fig. 1a and 1b). When a welding current of $Is = 280$ A was used, a relatively large penetration depth was observed (Fig. 1c and 1d), which may lead to increased material mixing with the substrate and reduced mechanical properties. Correct penetration depth across the entire bead width was observed for cases where the hardfacing current was higher than 220 A and the welding movement speed did not exceed 30 cm/min (Fig. 1c and d). Too deep penetration was achieved for a low welding speed of $Vs = 20$ cm/min, and localized lack of fusion was observed for a high welding speed of $Vs = 40$ cm/min. This allowed for the adoption of a narrow range of parameters, which were then experimentally verified during hardfacing (TABLE 3).

TABLE 3

Designated, main parameters process hardfacing forging tools

Material base	55NiCrMoV6
Pre-heat temp. heating up	250°C
Interpass temperature	max 400°C
Material additional	EnDOtec DO*04
current and voltage of current in hardfacing, method 138	$Isp = 260$ A $Ul = 28$ V
Speed movement handle welding	30 cm/min
Type and quantity gas protective	95% Ar + 5% CO_2 16-20 l/min
Treatment thermal after hardfacing	Annealing relaxing 540°C /2h
Parameters possible processing thermal	520 HV0.5

2.2.2. Complex model

Parameters obtained from the preliminary model were used to model the hardfacing of a complex-geometry matrix. Boundary conditions were applied in the model in the form of tool restraint to the welding table, which are shown in Fig. 2. Additionally, appropriate trajectories for the welding torch and

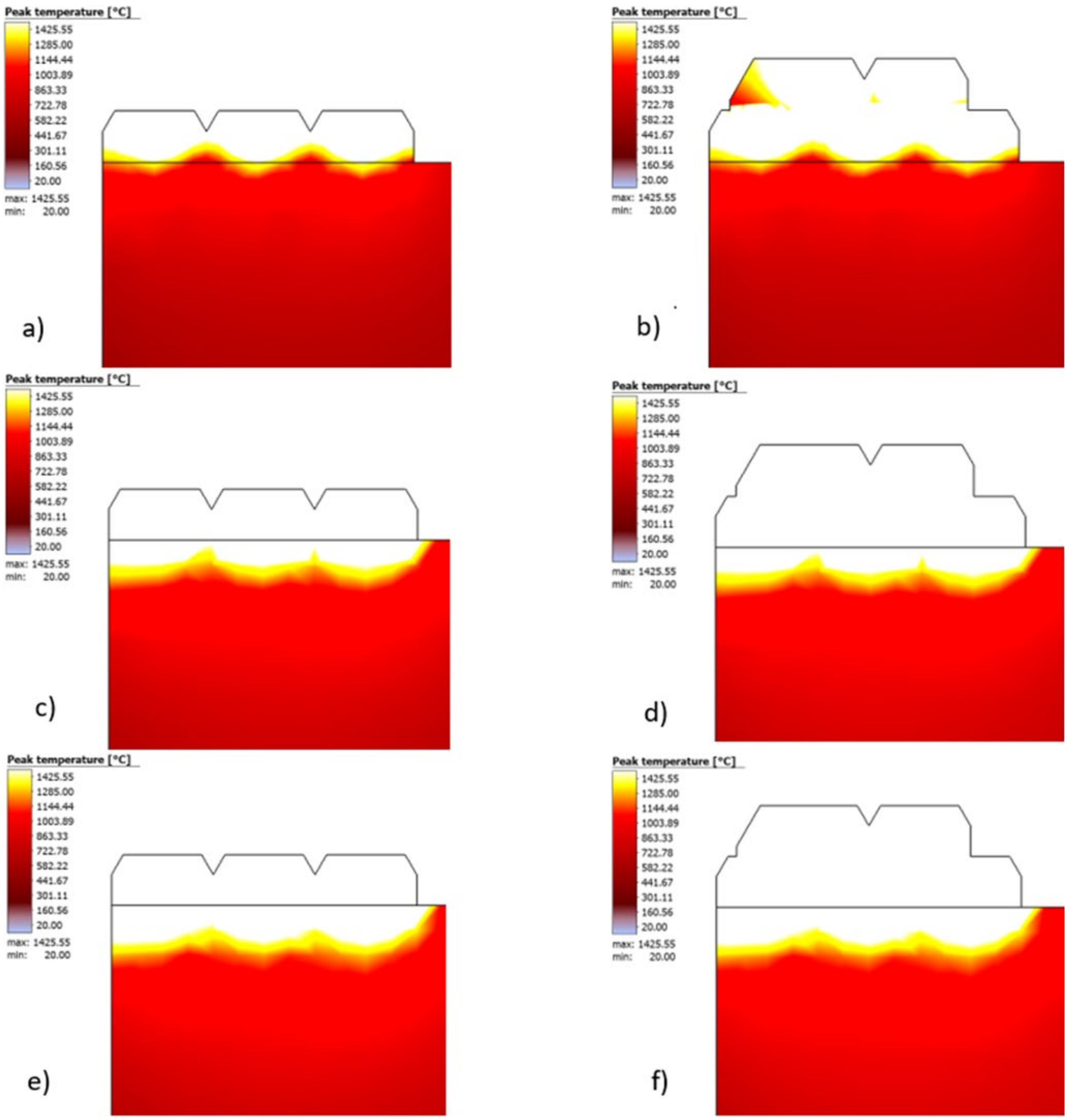

Fig. 1. Example schedules for temperature distribution for estimating the depth fusion: a) I layer welded Is = 180 A, b) II layer welded Is = 180 A, c) I layer welded Is = 220 A, d) II layer welded Is = 220 A, e) I layer welded Is = 280 A, f) II layer welded Is = 280 A

heat source were implemented in the form of a so-called double ellipsoid, based on the Goldak model. Simplifications were also applied to the weld geometry due to the model discretization process and the need to represent the welds using cubic finite elements (hexahedrons). Using overly complex weld geometries requires significant mesh refinement and an unreasonable increase in computation time. As observed in previous analyses, this does not significantly improve the model's quality or the results. Furthermore, during the calculations, a mesh refinement function (refinement) was applied at the heat source locations, which does not significantly increase the total number of finite elements in the model while significantly improving the quality of the obtained results. The model after applying the finite element mesh, along with the hardfacing trajectories, is shown in Fig. 2a, while the bead geometry and welding torch setup are shown in Fig. 2b.

The tool regenerative hardfacing station enabled the hardfacing process to be performed with assuming the welding positioner's movement (rotation or rotation with tilt) and the manipulation of the welding package by a robotic arm. This was also used in the welding process simulation in Simufact. Welding. Order of the weld beads is shown in Fig. 3. Welding began from the inner edge (bead 1), followed by subsequent weld beads, each with a correspondingly smaller diameter (beads 2 to 4). Once the

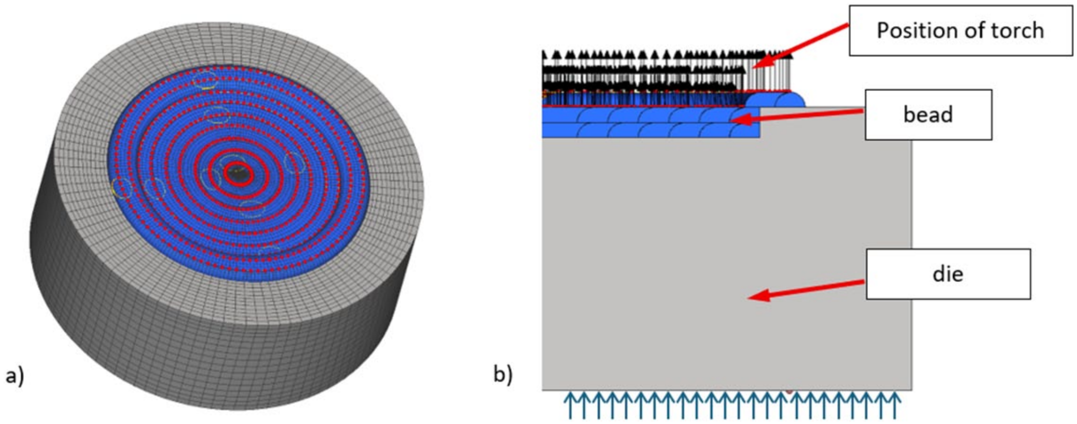

Fig. 2. Model of a cylindrical die: a) die geometry with trajectories, b) weld geometry in cross-section, blue arrows indicate the surface fixed to the welding table

cutout was completed to the inner undercut, weld beads were welded along the inner contour (beads 5 and 6). The layer was completed with the smallest diameter weld beads (beads 7 to *n*) to obtain a complete layer. Each subsequent weld bead was offset by a point angle of at least 15 degrees to avoid creating a crater depression in the same tool line. Subsequent layers were also rotated angularly relative to the previous ones.

2.3. Experiment

In the next stage of the process, an experiment was conducted to hardfacing a complex die geometry. The hardfacing process was recorded with a thermal imaging camera. The resulting image and the results of spot measurements are shown in Fig. 4. Using the thermal imaging camera allowed for monitoring the interpass temperature. It is crucial parameter in the hardfacing of tool steels. Furthermore, the cooling speed at selected spots of the die could be estimated. Thermal imaging measurements were selectively verified using thermocouple measurements to determine the correct emissivity coefficient.

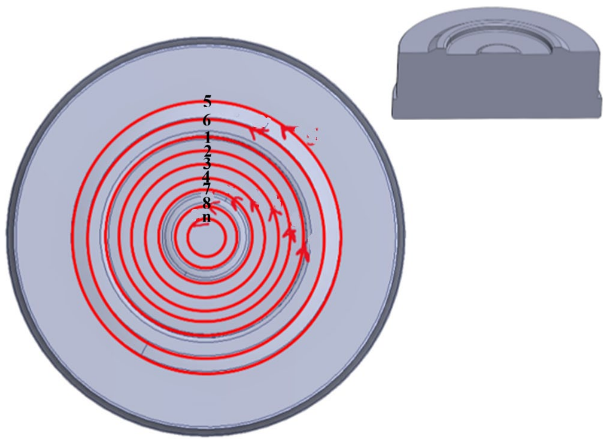

Fig. 3. The sequence of making beads in the first layer of the overlay for a tool with a cutout of complex geometry

2.4. Material research

In order to assess the quality of the performed regeneration, the tool was subjected to material tests. A sample was taken from

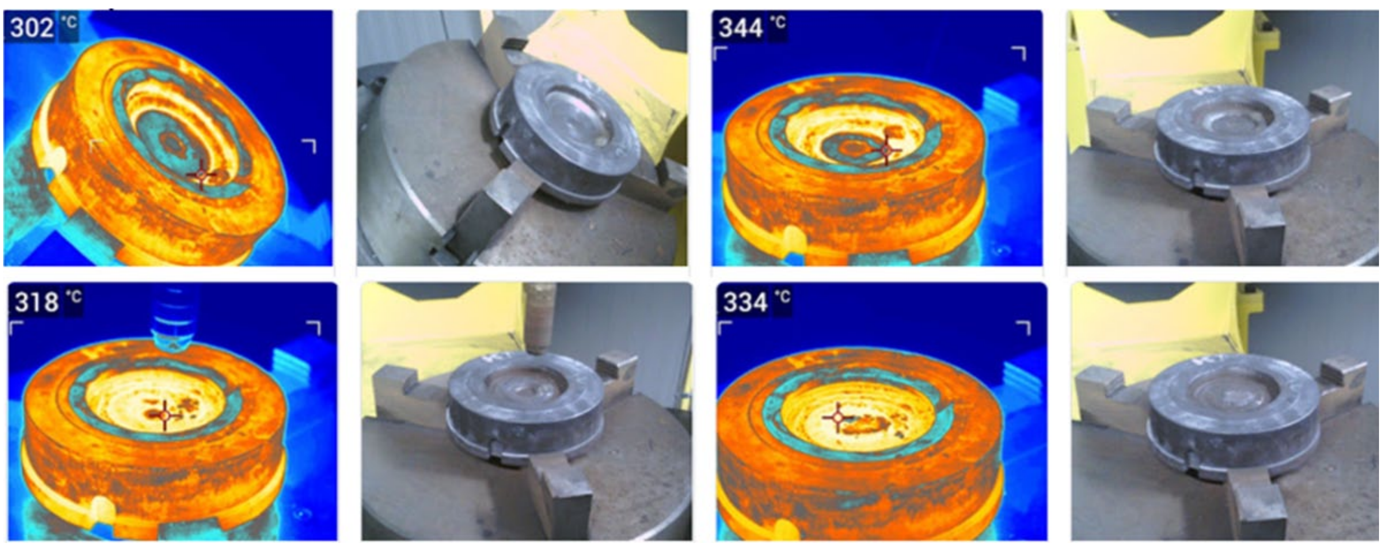

Fig. 4. Results of thermal imaging camera tests. Visible values of point temperature measurements on the tool surface

the tool for metallographic examination – using electro-erosion cutting. The location where the sample was taken for testing is shown in Fig. 5.

Fig. 5. Location of sampling for material testing

Microscopic examinations were performed on traditionally prepared metallographic samples. For that reason the cross- sections of the obtained weld deposits were prepared. Microstructure assessment was performed using the Leica DM6000M light microscope. The samples were etched using a solution of 3 ml picric acid (99.9%) in ethyl alcohol. Hardness measurements were performed using the Vickers method (Leco AMH55 hardness tester), at a load of 0.5 kgf (HV0.5).

3. Research results

In the next stage of the research, the results obtained from mathematical modeling were compared with experimental results. The model primarily enables the determination of temperature distribution during the hardfacing process, cooling rate, and hardness distribution in selected hardfacing areas (Fig. 6). Using this model and experimental studies, the usefulness of the developed methodology for analyzing the hardfacing process was verified.

EnDOtec DO*04 filler wire was used. Appropriate boundary and initial conditions were then implemented. The initial die temperature was 250°C. The welding current was 260 A and the welding speed was 30 cm/min. These conditions were selected to achieve a uniform bond between the passes and the die base material. The comparison of the hardfacing layer shapes from modeling and experiments is shown in Fig. 7.

Using the cooling rate data, the t8/5 times were determined, and based on these, the hardness distribution of the element after the hardfacing process was calculated (Fig. 8) using the Continuous Cooling Transformation for 55NiCrMoV6 steel [33]. After the hardfacing process, the welds reached approximately 480 HV0.5, according to modeling.

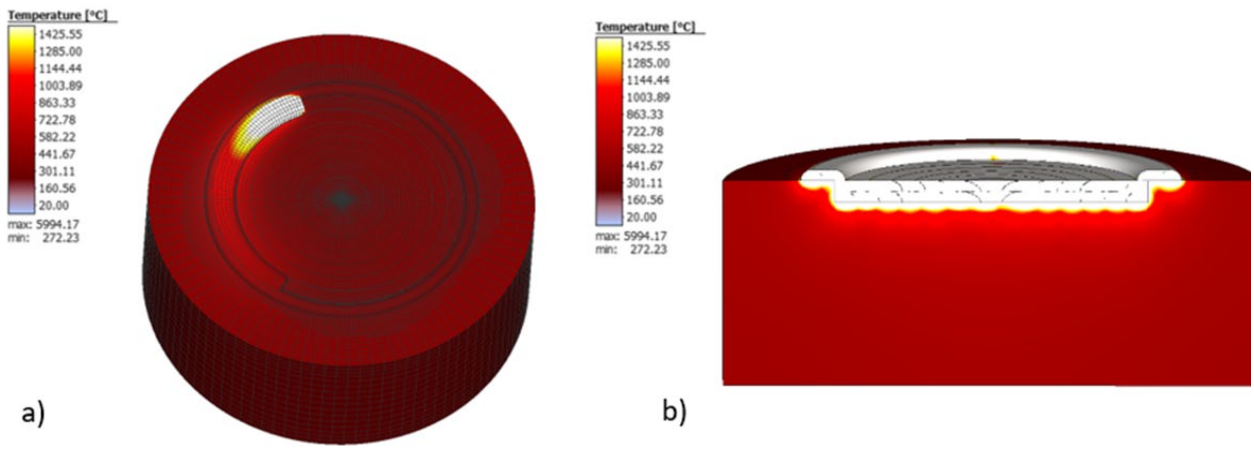

Fig. 6. Calculation results of the temperature distribution field: a) during hardfacing, b) maximum temperature in the cross-section of the die

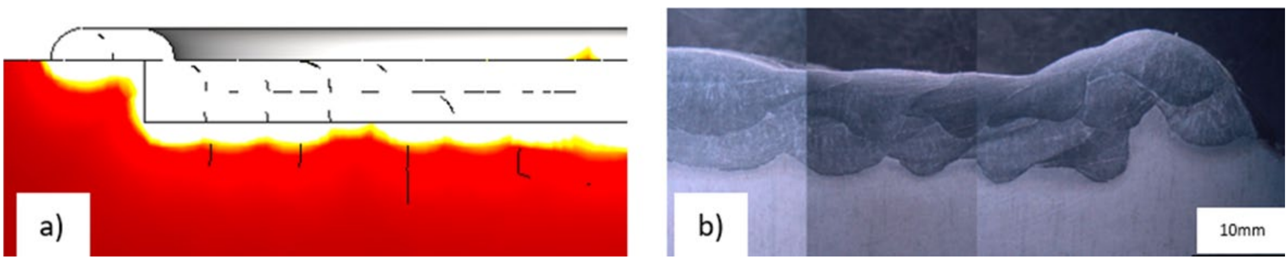

Fig. 7. Comparison of the results of FEM modeling and metallographic analysis: a) distribution of the maximum temperature during the hardfacing process, b) result of macrographic examination (depth of penetration and actual geometry of the hardfacing welds)

For the analyzed cylindrical die, a microhardness distribution measurement was performed to assess this parameter in the selected, most heavily loaded area of the die. The model after hardfacing was shown to be consistent with the hardness measurements in the experiment, as shown in Fig. 9.

In the experiment, the native material under the hardfacing welds was significantly hardened (over 600 HV0,5), which can lead to cracking. For this reason, the matrix is cooled "with the furnace" after the hardfacing process and then subjected to thermal heat treatment, involving tempering the element at approximately 540°C for 2 hours. After heat treatment the weld deposit reaches a hardness of at least 530 HV0.5.

This comparison confirms that the hardness distribution obtained from the model is close to the actual hardness test result. It should be noted that the material models were developed for HV0.5 hardness testing, and satisfactory agreement with the actual measurement was achieved, differences in hardness are less than 20% in significant regenerated areas. The microhardness distribution is very valuable information from a technological perspective. The data presented in Fig. 9 confirm the usefulness of the developed model also for assessing the microhardness distribution in the area of the weld and its immediate surroundings.

3.1. Results of metallographic tests

Metallographic examinations also included microscopic observations using light microscopy methods. Examples of

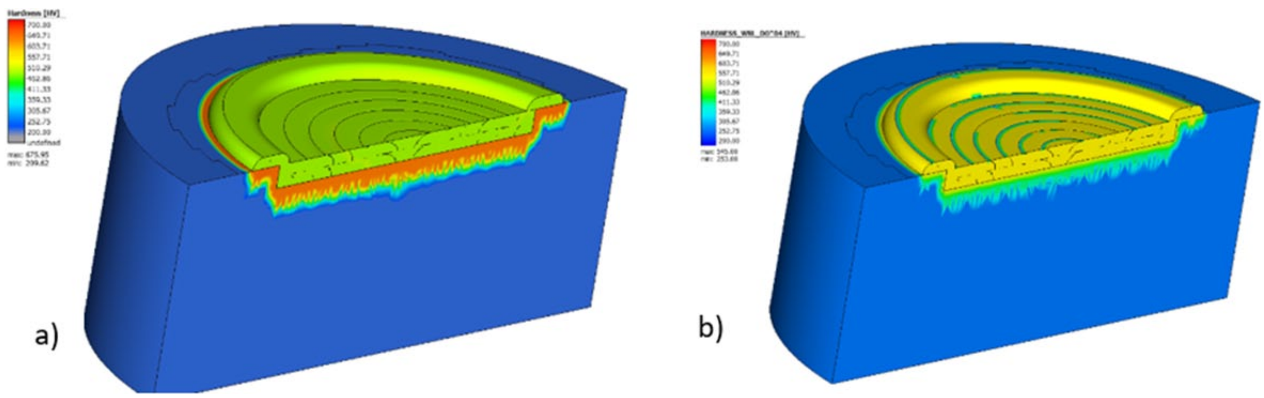

Fig. 8. Hardness test results: a) FEM model after hardfacing, b) FEM model after heat treatment

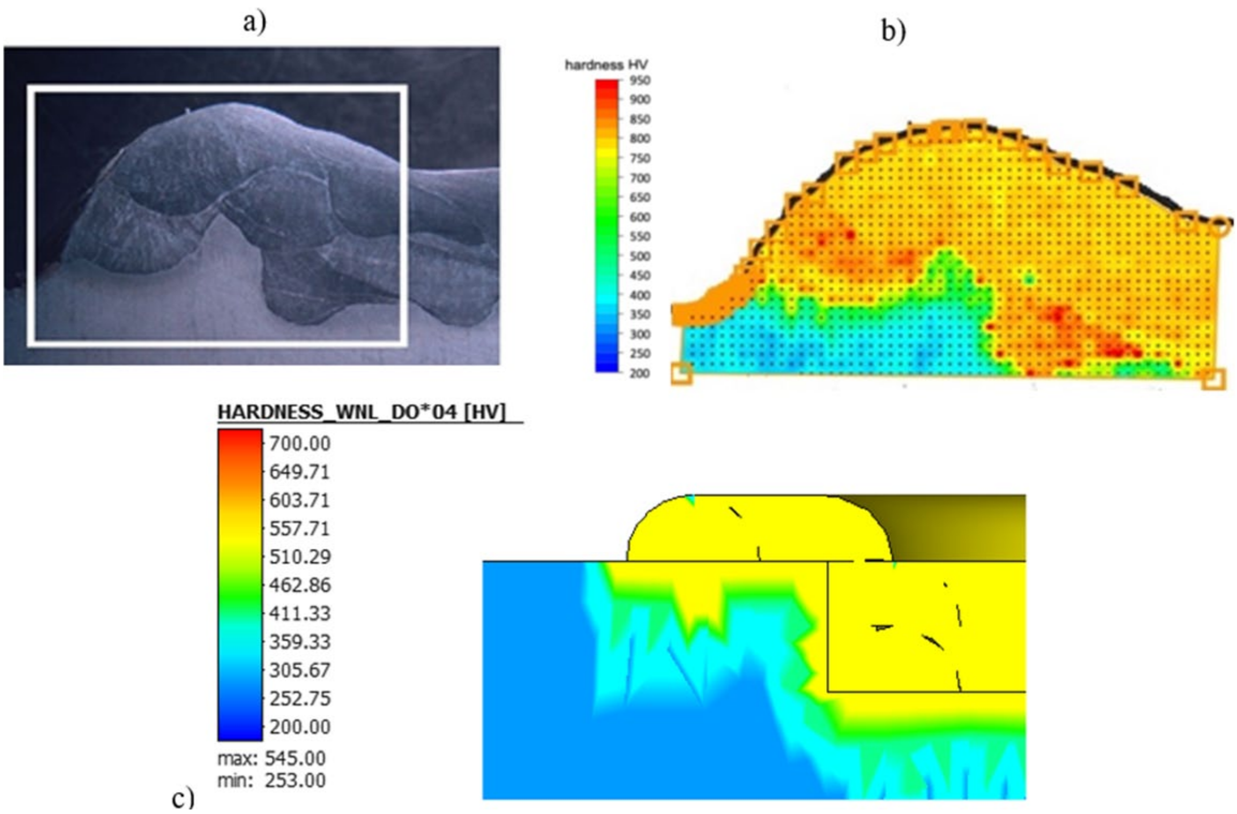

Fig. 9. Hardness test results: a) view of the macrostructure at the hardness measurement location, b) hardness in experiment – microhardness mapping, c) hardness based on the FEM model

microstructures obtained on the tested 55NiCrMoV6 steel using DO*04 as an additional material are shown in Figs. 10-12.

The partial melting zone demonstrated continuity between the parent material and the weld. Immediately behind it, an overheating (grain growth) zone was observed with a final microstructure of bainite, locally occurring with an increased content of untransformed austenite (Fig. 10). It should be noted that despite the good hardenability of 55NiCrMoV6 steel, the bainite content in this region is significantly influenced by the tool thickness. The typical cooling rate in open air is assumed to be between 0.5 and 1.5°C/s, depending on the component thickness. Therefore, for components with larger cross-sections, the estimated time to reach a temperature of 500°C in the austenitization range may exceed 10 minutes, which is sufficient for the bainitic transforma-

a)

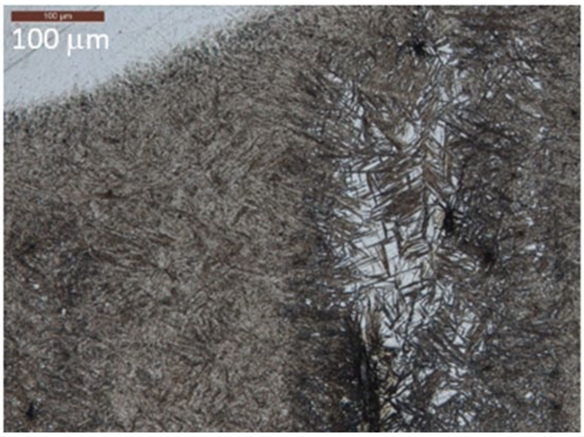

b)

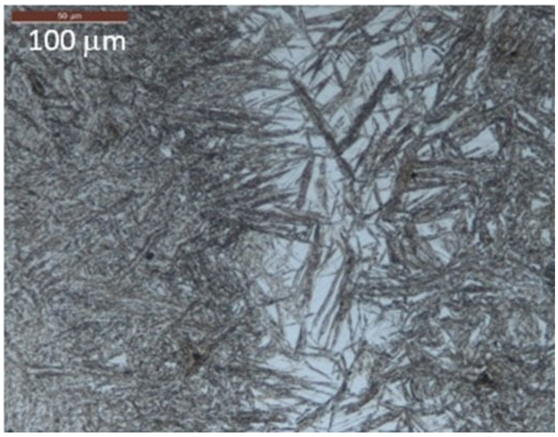

Fig. 10. a) Microstructure of the weld obtained on a 55NiCrMoV6 steel tool using DO*04 filler material in the overheated heat-affected zone area and b) enlarged fragment of the area from figure a. Light microscopy, etched state

a)

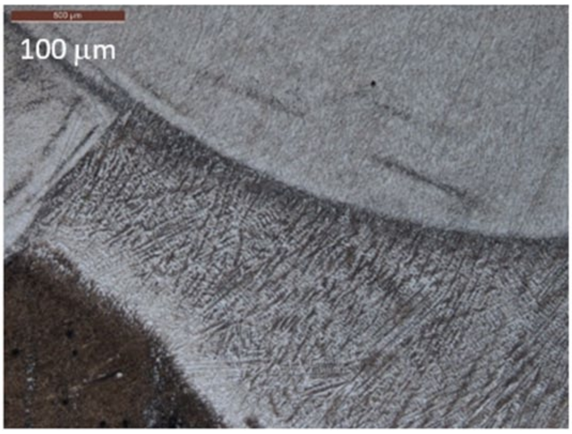

b)

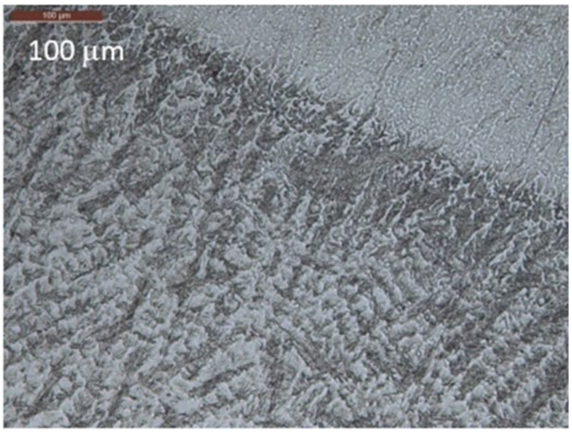

Fig. 11. a) Microstructure of the hardfacing weld obtained on a 55NiCrMoV6 steel tool using DO*04 filler material. b) Enlarged fragment of the area from figure a. Light microscopy, etched state

a)

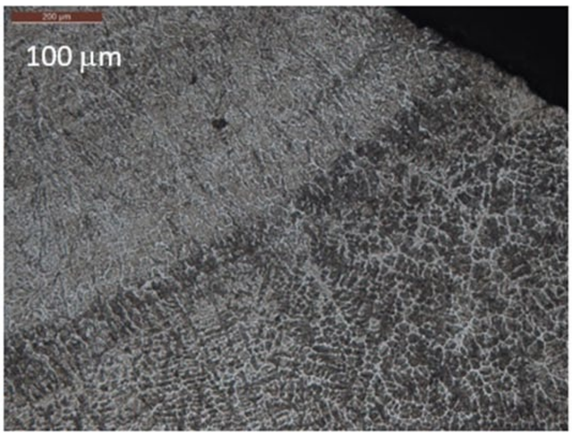

b)

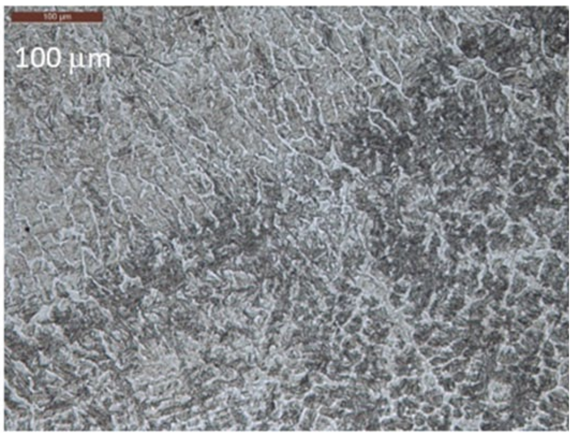

Fig. 12. a) Microstructure of the overlay obtained on a 55NiCrMoV6 steel tool using DO*04 filler material in the near-surface area. b) Enlarged fragment of the area from figure a. Light microscopy, etched state

tion to occur. The greater the component thickness, the longer this time, which translates into an increasing amount of bainite in the microstructure.

With increasing distance from the weld overlay, grain size is normalized within the HAZ. Directly adjacent to the parent material, a zone was located associated with the temperature range close to the AC1 line on the iron-cementite diagram. Transformations associated with tempering of the parent material were observed in this zone. A martensitic-bainitic microstructure was observed in the weld overlay area, with the bainite content decreasing with increasing distance from the substrate material. As can be seen from the CCT diagram, the presence of bainite does not result in a significant decrease in hardness in this steel, which explains the stability of hardness in individual areas of the weld overlay, despite significant variations in martensite content. In the last layer of the weld overlay, a predominantly martensitic microstructure with a dendritic crystallization front was observed (Figs. 11 and 12).

The microscopic examinations are consistent with the hardness distribution for this weld, as shown in Fig. 11b. As can be seen, the hardness in the weld area was approximately 750 HV0.5. The highest local hardness, reaching nearly 900 HV0.5, was observed in the first layer, which is attributed to the mixing of the filler material with the substrate material. This resulted in an increase in carbon content and the observed increase in hardness in this area. Detailed changes in the element distributions and their impact on hardness are presented in the paper [34]. Additionally, this effect could be intensified by secondary hardness induced by alloying elements in the parent material, as subsequent layers are heated during the hardfacing of earlier-deposited layers. In particular, the presence of molybdenum in the chemical composition of the tool steel may have contributed to this. Immediately behind the weld, directly behind the fusion line, the hardness of the parent material was approximately 500 HV0.5. Next, an area of distinct "softening" of the material was observed, caused by changes associated with tempering at high temperatures (impact of the heat of hardfacing). This area was followed by a transition to the hardness characteristic of the native material (no effect of temperature on structural changes).

4. Summary and conclusions

- The use of FEM modeling of the hardfacing process enabled the analysis of a wide range of process parameters and their influence, mainly on the penetration depth.
- Correct penetration depth across the entire bead width was observed for cases where the hardfacing current was higher than 260 A and the welding movement speed did not exceed 30 cm/min.
- The simulation of the forging die hardfacing process allowed for narrowing the scope of the search for individual parameters, which directly influenced the time and number of experimental tests performed.
- Based on the created numerical model, the hardness distribution of the welded layers was estimated, which made it possible to determine their suitability for forging processes and to assess the machining possibilities of the die work surface.
- After the hardfacing process, the hardfacing welds reached approximately 480 HV0,5. Native material under the hardfacing welds was significantly hardened (over 600 HV0,5), which can lead to cracking. For this reason, the matrix is cooled „with the furnace“ after the hardfacing process and then subjected to thermal heat treatment involving tempering the element at a temperature of approximately 540°C for 2 hours. After heat treatment the weld deposit reaches a hardness of at least 530 HV0.5.

REFERENCES

[1] P. Lisiecka-Graca, Ł. Lisiecki, K. Zyguła, M. Wojtaszek, Evaluation of the possibility of improving the durability of Evaluation of cracking risk of 80MnSi8-6 nanobainitic steel during hot forging in the range of lower temperature limits. Materials Science- Poland **42,** 171-185(2024).
DOI: https://doi.org/10.2478/msp-2024-0011

[2] M. Hawryluk, Tribological performance of Orvar 2M tool steel coated with ALWIN XC for improved forging tool durability. Materials Science-Poland **43**, 107-121 (2025).
DOI: https://doi.org/10.2478/msp-2025-0045

[3] P. Widomski, Z. Gronostajski, Comprehensive review of methods for increasing the durability of hot forging tools. Procedia Manuf. (2020).

[4] M. Wojtaszek, G. Korpała, K. Zyguła, K. Cichocki, K. Kowalczyk, W. Skonieczna, B. Mrzygłód, U. Prahl, M.B. Jabłońska, Fuzzy logic as a method of analysis of hot forging process of 80MnSi8-6 steel. Archives of Civil and Mechanical Engineering **25** (2025).
DOI: https://doi.org/10.1007/s43452-024-01088-0

[5] B.A. Behrens, Finite element analysis of die wear in hot forging processes. CIRP Ann. Manuf. Technol. (2008).
DOI: https://doi.org/10.1016/j.cirp.2008.03.087

[6] M. Hawryluk, Ł. Dudkiewicz, M. Jabłońska, S. Polak, J. Marzec, Analysis of the destruction of a die insert used in the industrial process of hot die forging to produce a yoke forging. Eng. Fail. Anal. **164** (2024).
DOI: https://doi.org/10.1016/j.engfailanal.2024.108661

[7] M.M. Lachowicz, Insight into the microstructural stability and thermal fatigue behavior of nitrided layers on martensitic hot forging tools. Materials Science-Poland **43**, 1-17 (2025).
DOI: https://doi.org/10.2478/msp-2025-0005

[8] J.H. Kang, I.W. Park, J.S. Jae, S.S. Kang, Study on die wear model considering thermal softening (II): Application of the suggested wear model. J. Mater. Process. Technol. **94**, 183-188 (1999).
DOI: https://doi.org/10.1016/s0924-0136(99)00104-1

[9] J. Krawczyk, P. Widomski, M. Kaszuba, Advanced Complex Analysis of the Thermal Softening of Nitrided Layers in Tools during Hot Die Forging. Materials **14**, 355 (2021).
DOI: https://doi.org/10.3390/ma14020355

[10] C. Wu, W. Li, Z. Tang, J. Liang, J. Li, Effect of laser welding on the microstructure and properties of ultrathin Inconel 718 sheets. Materials Science-Poland **43**, 153-170 (2025). DOI: https://doi.org/10.2478/msp-2025-0026

[11] M. Górnik, M. Lachowicz, L. Łatka, Corrosion resistance of PPTA Ni-based hardfacing layers. Materials Science-Poland **42**, 66-78 (2024). DOI: https://doi.org/10.2478/msp-2024-0040

[12] B. Buchmayr, Damage, Lifetime, and Repair of Forging Dies, BHM Berg- Und Hüttenmännische Monatshefte **162**, 88-93 (2017). DOI: https://doi.org/10.1007/s00501-016-0566-3

[13] P. Widomski, M. Kaszuba, P. Sokołowski, A. Lange, M. Walczak, M. Długozima, M. Gierek, D. Chocyk, G. Gładyszewski, B. Boryczko, Nitriding of hardfaced layers as a method of improving wear resistance of hot forging tools, Archives of Civil and Mechanical Engineering **23**, 241(2023). DOI: https://doi.org/10.1007/s43452-023-00778-5

[14] R. Miller, Weld Repair of Tools and Dies: 10 Popular Q&As, Postle Industries, Inc.; Cleveland, Ohio (2017) 1-3. http://www.hardfacetechnologies.com/postle_hft_btsp/pdfs/forge-weld-repair-postle.pdf

[15] V. Lazić, A. Sedmak, S. Aleksandrović, D. Milosavljević, R. Čukić, V. Grabulov, Reparation of the damaged forging hammer mallet by hard facing and weld cladding. Tehnicki Vjesnik (2009).

[16] Investigating the Possibility of Regenearation by Hardfacing for Forging Tools Based on Analysis of Tool Working Conditions and Wear Evaluationy. Archives of Metallurgy and Materials (2023). DOI: https://doi.org/10.24425/amm.2022.141067

[17] D. Lee, Extend Die Life with Flood Welding. (2019). https://www.forgemag.com/articles/84887-extend-die-life-with-flood-welding (accessed April 12, 2020).

[18] C.U. Balu, P.O. Daijo, K.P.S. Faizal, T.O. Rinson, J. Salim, Sigimon, T. Mathew, Welding life enhancement of steel forging dies. International Journal of Advanced Engineering and Global Technology **4**, 1771-1779 (2016).

[19] H. Kashani, A. Amadeh, M.R. Vatanara, Improvement of wear resistance of hot working tool steel by hardfacing. Part 2 – Case study. Materials Science and Technology **24**, 356-360 (2008). DOI: https://doi.org/10.1179/174328407x166731

[20] D.G. Ahn, H.J. Lee, J.R. Cho, D.S. Guk, Improvement of the wear resistance of hot forging dies using a locally selective deposition technology with transition layers. CIRP Ann. Manuf. Technol. **65**, 257-260 (2016). DOI: https://doi.org/10.1016/j.cirp.2016.04.013

[21] D.I. Kim, Y.H. Jang, H.J. Lee, D.G. Ahn, H. Song, C.S. Seok, Design of overlay coated region with hardfacing, transition and damage diminution layers for the reduction of damages of hot forging tools. Journal of Mechanical Science and Technology **31**, 5639-5647 (2017). DOI: https://doi.org/10.1007/s12206-017-1104-2

[22] F. Gao, J. Zhou, J. Zhou, L. Shen, J. Zhang, Y.P. Tao, M.Y. Li, Microstructure and properties of surfacing layers of dies manufactured by bimetal-gradient-layer surfacing technology before and after service. International Journal of Advanced Manufacturing Technology (2017). DOI: https://doi.org/10.1007/s00170-016-8679-0

[23] L. Shen, J. Zhou, Y.B. Xiong, J.S. Zhang, Y. Meng, Analysis of service condition of large hot forging die and refabrication of die by bimetal-layer weld surfacing technology with a cobalt-based superalloy and a ferrous alloy. J. Manuf. Process. (2018). DOI: https://doi.org/10.1016/j.jmapro.2018.01.005

[24] Y.-H. Lü, Y.-X. Liu, F.-J. Xu, B.-S. Xu, Plasma transferred arc forming technology for remanufacture. Adv. Manuf. **1**, 187-190 (2013). DOI: https://doi.org/10.1007/s40436-013-0017-2

[25] P. Widomski, M. Kaszuba, M. Zwierzchowski, C. Goulas, M. Bos, M. Hermans, WAAM-based repair cladding for forging tools: a comprehensive study of wear in laboratory and industrial conditions. Archives of Civil and Mechanical Engineering **26**, 84 (2026). DOI: https://doi.org/10.1007/s43452-026-01461-1

[26] V. Pusateri, S.I. Olsen, LCA and LCC of wire arc additively manufactured and repaired parts compared to conventional fabrication techniques. Procedia CIRP **122**, 491-496 (2024). DOI: https://doi.org/10.1016/j.procir.2024.01.071

[27] M. Kaszuba, P. Widomski, T. Kiełczawa, Z. Gronostajski, The use of a measuring arm with a laser scanner for analysis and support of regenerative surfacing processes of forging dies. Welding Technology Review **92**, 23-32 (2020).

[28] Aref Abadel, Shear strengthening of deficient RC deep beams using NSM FRP system: Experimental and numerical investigation. Materials Science- Poland **42**, 140-157 (2024). DOI: https://doi.org/10.2478/msp-2024-0012

[29] S. Liu, Z. Wu, W. Zhou, H. Zhou, K. Zhang, D. Yin, Y. Lei, Y. Qiu, A review of welding simulation methods for large components. Progress in Natural Science: Materials International **33**, 551-568 (2023). DOI: https://doi.org/10.1016/j.pnsc.2023.12.004

[30] M. Wojtaszek, Ł. Lisiecki, A. Łukaszek-Sołek, G. Korpała, K. Zyguła, T. Śleboda, M.B. Jabłońska, U. Prahl, Application of processing maps and numerical modelling for identification of parameters and limitations of hot forging process of 80MnSi8-6 steel. Archives of Civil and Mechanical Engineering **23** (2023). DOI: https://doi.org/10.1007/s43452-023-00783-8

[31] L.D. Meléndez-Morales, J.J. Ruíz-Mondragón, M. Hernández-Hernández, In-service weld repair by direct deposition: Numerical simulation and experimental validation, Engineering Science and Technology. an International Journal **46**, 101503 (2023). DOI: https://doi.org/10.1016/j.jestch.2023.101503

[32] C. Deng, W. Chen, Y. Zhu, Multi-Physics Modeling in Curved Surface Laser Cladding: Impact of Scanning Trajectories and Cladding Parameters on Temperature Field and Coating Thickness. Crystals (Basel). **15**, 128 (2025). DOI: https://doi.org/10.3390/cryst15020128

[33] L. Habraken, J.-L. de Brouwer, De ferri metallographia: Grundlagen der Metallographie, Presses Academiques Europeans S.C. Bruxelles, 1966.

[34] M.M. Lachowicz, P. Sokołowski, M. Kaszuba, The Influence of the Hot Working Tool Steel Substrate Material on the Element Distribution, Microstructure and Hardness of Gas Metal Arc Welding Hardfaced Layers. Advances in Science and Technology Research Journal **18**, 320-333 (2024). DOI: https://doi.org/10.12913/22998624/181188